High T_e, low collisional plasma confinement characteristics in LHD

H. Takahashi 1), T. Shimozuma 1), S. Kubo 1), I. Yamada 1), S. Muto 1), M. Yokoyama 1), H. Tsuchiya 1), T. Ido 1), A. Shimizu 1), C. Suzuki 1), K. Ida 1), S. Matsuoka 2), S. Satake 1), K. Narihara 1), N. Tamura 1), Y. Yoshimura 1), H. Igami 1), H. Kasahara 1), Y. Tatematsu 3), T. Mutoh 1) and the LHD experiment group 1)

1) National Institute for Fusion Science, Toki 509-5292, Japan
2) The graduate University for Advanced Studies, Toki 509-5292, Japan
3) Research Center for Development of Far-Infrared Region, University of Fukui, Fukui, 910-8507, Japan

E-mail contact of main author: takahashi.hiromi@LHD.nifs.ac.jp

Abstract. High electron temperature (T_e) plasmas of more than 15 keV were achieved due to the upgraded electron cyclotron resonance heating system with newly installed 77 GHz-over 1 MW gyrotrons in the Large Helical Device. The value of T_e greatly exceeds ~10 keV, which was obtained in previous experiments. The configuration dependence of high T_e plasma performance was investigated under the magnetic field strength of ~2.7 T and the optimum configuration for achieving high T_e plasma was observed. These high T_e plasmas accompanied an electron internal transport barrier (e-ITB). Clear threshold of density-normalized ECRH power for an e-ITB formation was found. The foot point of an e-ITB moved outward during ECRH injection and the flat T_e profile gradually healed with the propagation of the e-ITB foot point. The foot point finally reached to a lower order rational surface of $\iota/2\pi = 0.5$.

1. Introduction

An electron internal transport barrier (e-ITB) is characterized by a steep gradient formation in an electron temperature profile, a formation of a strong radial electric field (and/or its shear) and a decrease in an electric thermal diffusivity in a plasma core region [1, 2]. Up to now, this improved mode has been observed in several devices and has been intensively investigated [3-6]. There is a hypothesis based on some experimental results that lower-order rational surfaces or a local minimum of a safety factors play a important role for an e-ITB formation in both tokamaks and helical devices [1, 7-10]. One of the key issues for the e-ITB study is to clarify an effect of a rotational transform on an e-ITB formation.

Since 2006, the installation of 77 GHz gyrotrons with each output power of over 1 MW has progressed in the Large Helical Device (LHD) [11]. These high power gyrotrons enabled us to achieve a higher electron temperature (T_e) than that previously obtained [12] and also to survey properties of high T_e plasmas in wide configuration range due to the oscillation frequency selected as 77 GHz, which is different from those of the gyrotrons already installed in the LHD. Such low collisional plasmas are suitable for an investigation of a configuration effect on plasma characteristics in toroidal systems. One of the important advantages of electron cyclotron resonance heating (ECRH) is that perpendicularly injected ECRH can produce plasmas without driven toroidal current. A mechanism of an e-ITB formation relating with lower order rational surfaces has been studied in LHD [10, 13]. Most of the previous e-ITB experiments were carried out using centre-focused ECRH overlapping to plasmas sustained by neutral beam injection (NBI). There were always effects of inductive return current against NBI driven current on the position of the rational surface because the relaxation time of the return current in LHD is several seconds, which is generally longer than the plasma sustainment time [14]. Thus it becomes possible to investigate the dynamics of e-

ITB formation and the relation between the foot point and the lower-order rational surfaces without the effect of return current by using high-power ECRH alone.

2. Experimental Setup

The LHD is the largest heliotron device with R = 3.9 m, a = 0.6 m, and has a pole number of 2 and a toroidal period of 10 [15]. The heliotron configurations are produced by a set of helical winding coils and three sets of poloidal field coils, which are all superconducting magnets. The magnetic field on the axis is ~2.9 T. In the LHD, an ECRH system with eight gyrotrons, whose frequencies are 77 (the new tube developed through the joint program with Tsukuba University, JAEA and Toshiba Electron Tubes & Devices; TETD), 82.7 (Gycom), 84 (Gycom) and 168 GHz (TETD), has been operated for preionization and plasma heating [16]. Of these, the high power 77-GHz gyrotrons with the output power of more than 1 MW have been operated since the 11th experimental campaign. Figure 1 (a) shows the history of ECRH port-through power. In the present state, three 77 GHz gyrotrons are operational for plasma experiments. The total injection power of ECRH to the plasma significantly increased due to the installation of the 77 GHz tubes and reached a value of 4 MW. The actual value of the simultaneous injection power to LHD is slight small (~3.7 MW) because the total input power for the gyrotrons is limited by the power capacity of the transformer. The poloidal magnetic surfaces with the injected electron cyclotron (EC) wave beams are illustrated in Fig.1 (b) and (c) for the magnetic configuration of R_{ax} = 3.75 m, B_t = 2.75 T. The EC wave beams are injected to plasma from upper, lower and horizontal antennas. In the cases that the resonance surfaces do not exist around the plasma centre in the horizontally-elongated surface as 168-GHz beam shown in Fig. 1 (c), the horizontally-injected beams are focused on the plasma axis in the vertically-elongated surface by toroidally oblique injection.

However a Thomson scattering system is one of the most reliable diagnostics for T_e measurement in toroidal devices, error bars of T_e data sometimes become large for high-T_e, low-n_e discharges due to the low intensity of the scattered light. In order to improve an accuracy of T_e data, we carried out discharges with the fixed parameters such as T_e and n_e to accumulate the Thomson scattered light and three YAG lasers firing all together to increase the scattered light intensity [17]. Figure 2 shows the dependence of T_e error on the accumulation number of the discharges. The T_e error is normalized by the value for n = 1. The open squares indicate the case of only one YAG laser firing as the usage for regular experiments and the solid squares are those of three lasers firing. As can be seen from Fig. 2, T_e error decreases with the dependence of $1/n^{-0.5}$. Three lasers firing was more effective and

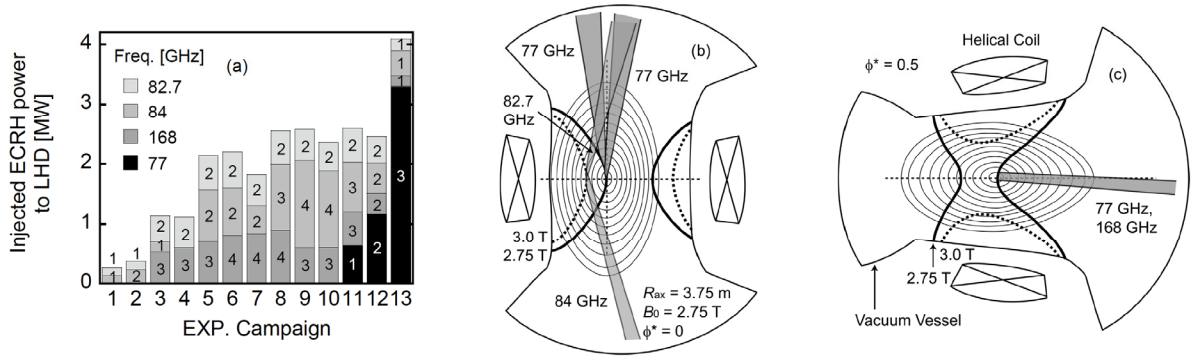

FIG. 1. (a) the history of ECRH port-through power, the injected EC wave beams in (b) the vertically and (c) the horizontally elongated magnetic surface for the magnetic configuration of R_{ax} = 3.75 m, B_t = 2.75 T.

highly accurate T_e could be successfully obtained by lesser discharge accumulation compared with the single laser firing. For steady state plasmas, T_e error can be decreased by time frame accumulation too. These technical methods for the improvement of T_e measurement accuracy is summarized in Ref [17].

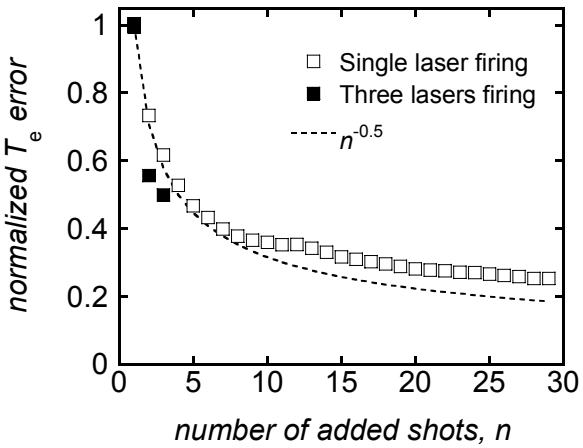

FIG. 2. The dependence of T_e error on the accumulation number of fixed discharges.

3. Configuration dependence

In the LHD, the configuration dependence of the confinement property has been studied and it has been pointed out the inward-shifted configuration R_{ax} = 3.53 m is optimum from the view point of neoclassical transport [18]. This was experimentally examined in the previous experiments for the low collisional plasmas (T_e ~1.5 keV, $0.3 \le n_e \le 1.5\times10^{19}$ m^{-3}) produced by ECRH alone [19]. In the present research, much lower collisional plasmas were treated and it was expected that the neoclassical characteristics for the plasma confinement emerges more clearly. We started from the configuration optimization for the production of high T_e plasmas.

Figure 3 shows (a) the radial profiles of T_e for three configuration cases; (R_{ax}, B_0) = (3.53 m, 2.705 T), (3.60 m, 2.705 T) and (3.75 m, 2.75 T) with approximately same electron density of n_e ~0.4×10^{19} m^{-3} and same injection power of P_{ECRH} ~2.7 MW, the dependence of (b) the central electron temperature T_{e0} and (c) R_{ax}/L_{Te} on R_{ax}, where R_{ax} is magnetic axis position, B_0 is the magnetic field on axis, L_{Te} is the radial scale length of T_e and R_{ax}/L_{Te} represents a performance of an e-ITB. The data in Fig.3 (b) and (c), n_e was approximately same value of ~0.5×10^{19} m^{-3} but P_{ECRH} was different. L_{Te} were evaluated at r_{eff}/a_{99} = 0.2, where r_{eff} is the effective minor radius and a_{99} is the averaged minor radius where the 99 % of the stored energy is confined. The plasmas were produced and sustained only by centre-focused ECRH. As can be seen from Fig. 3, the steepest profile and the highest T_{e0} were obtained for R_{ax} = 3.53 m. R_{ax}/L_{Te} for R_{ax} = 3.53 m was 1.5 times larger than that for the other configurations.

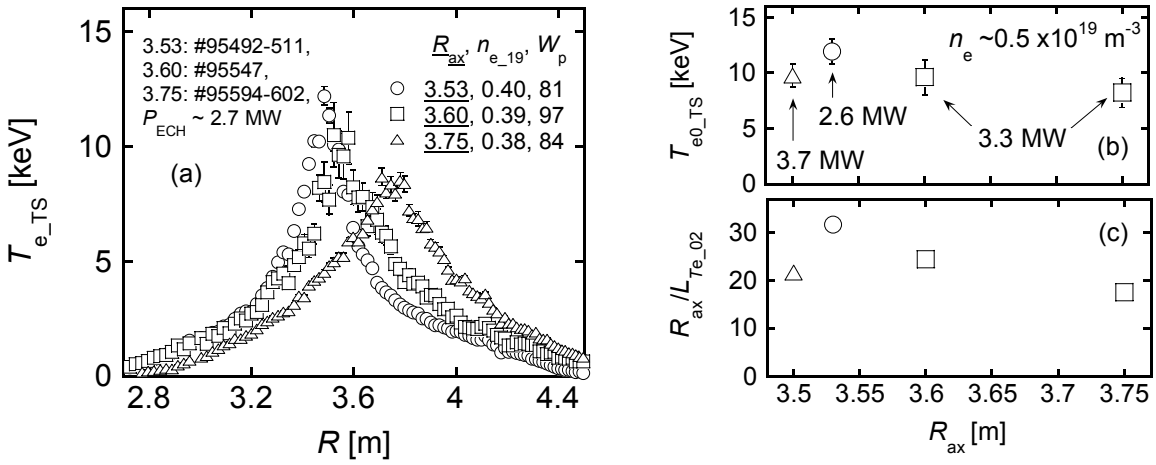

FIG. 3. (a) the radial profiles of T_e for three configuration cases; (R_{ax}, B_0) = (3.53 m, 2.705 T), (3.60 m, 2.705 T) and (3.75 m, 2.75 T), the configuration dependence of (b) the central electron temperature T_{e0} and (c) R_{ax}/L_{Te}.

PHA, SXCCD and ECE measurement showed that there was a certain amount of superthermal electrons in these high T_e, low collisional plasmas [20]. However, we have already confirmed that there was only small effect of the superthermal electrons for the bulk plasma temperature evaluation by the Thomson scattering measurement [17]. We confirmed that the superthermal electrons tend to be produced when an ECRH was obliquely injected to plasma. An increase of superthermal electrons may decrease the deposition power to bulk plasma because a part of the ECRH power is used for the production and/or the acceleration of the superthermal electrons.

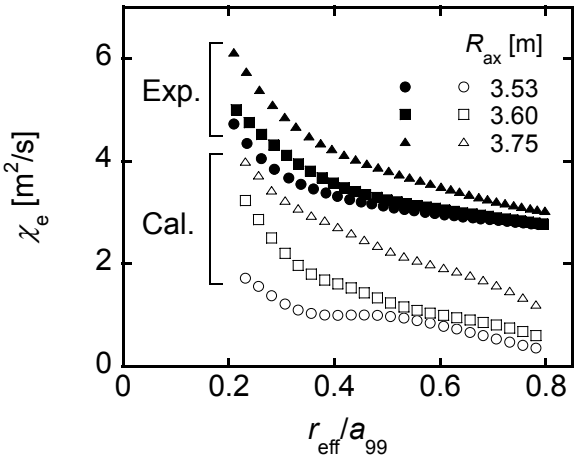

FIG. 4. The radial profiles of χ_e for the three cases in Fig. 3 (a).

We experimentally evaluated the electron thermal diffusivity χ_e and compared with the neoclassical one calculated using GSRAKE code, which solves the ripple-averaged drift kinetic equation [21, 22]. Figure 4 shows the radial profiles of χ_e for the three cases in Fig. 3 (a). The solid and open symbols represent the experimental and calculated χ_e, respectively. The experimental χ_e was simply obtained as $-P_{ECRH}/(Sn_e\partial T_e/\partial r_{eff})$ under the assumption that the energy transfer to the ion was negligible and the plasma was in steady state, where S is the area of the toroidal surface. The tendency of the experimental χ_e behaviour qualitatively agree with that of the calculation and the lowest χ_e values were obtained for the configuration of R_{ax} = 3.53 m in both experiments and calculation. Thus R_{ax} = 3.53 m is thought to be better configuration for an achievement of higher T_e plasmas in the LHD. This result is consistent with previous studies reported in Ref [18, 19].

4. Characteristic of e-ITB formation

Here we investigated a criterion of an e-ITB transition and the formation process of the e-ITB structure for a high T_e, low collisional plasma. Figure 5 shows the radial profiles of (a) T_e for four n_e cases; 0.23, 0.50, 0.73, 0.77×10^{19} m^{-3} and (b) the radial electric field E_r calculated

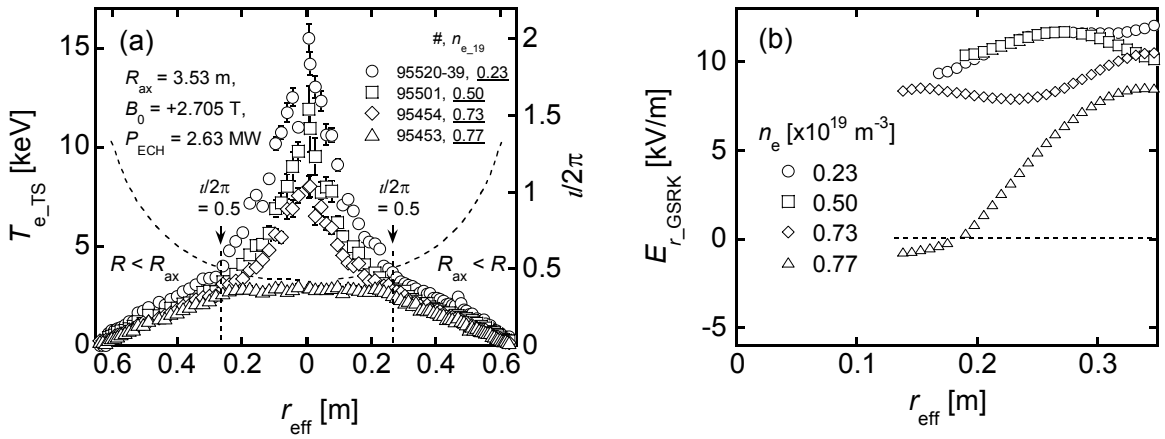

FIG. 5. The radial profiles of (a) T_e for four n_e cases; 0.23, 0.50, 0.73, 0.77×10^{19} m^{-3} and (b) the radial electric field E_r calculated using the GSRAKE code.

using the GSRAKE code. The rotational transform ($\iota/2\pi$) profile for a vacuum condition is also attached in Fig. 5 (a). Clear n_e threshold (and/or P_{ECRH}/n_e threshold) for the formation of the e-ITB was observed. The T_e profile drastically changed from flat to peaked one in the narrow range of $0.73 \le n_e \le 0.77\times10^{19}$ m^{-3}. Both the shoulder point of the flat T_e profile and the foot point of the e-ITB located at r_{eff} ~0.27 m and were coincident with the rational surface of $\iota/2\pi$ = 0.5. In Figure 5 (b) it is found that the positive E_r formation at the core region in the peaked T_e profiles and the core electron root confinement, which is improved confinement regime specific in helical plasmas [23] was achieved. On the other hand, E_r for the case of n_e ~0.77×10^{19} m^{-3} was negative and the absolute value was considerably smaller than those of the other three. We also experimentally observed the positive E_r formation by the heavy ion beam probe measurement [24] for the peaked T_e discharges. Figure 6 shows the dependence of T_{e0} on density-normalized ECRH power (P_{ECRH}/n_e) for R_{ax} = 3.53 m, B_0 = 2.705 T. All these plasmas were produced and sustained by ECRH alone. Clear threshold of P_{ECRH}/n_e for the formation of the e-ITB was found. Once the e-ITB formed, T_{e0} increased with the proportional dependence of ~$(P_{ECRH}/n_e)^{0.5}$. Finally more than 15 keV of T_{e0} was successfully achieved for low n_e plasmas ($n_e \le 0.23\times10^{19}$ m^{-3}).

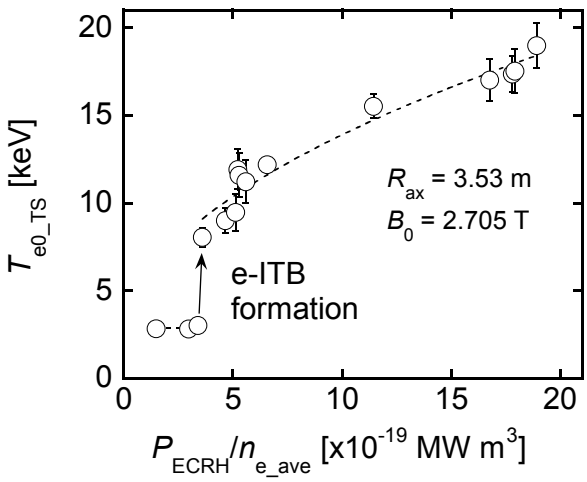

FIG. 6. the dependence of T_{e0} on density-normalized ECRH power for R_{ax} = 3.53 m, B_0 = 2.705 T.

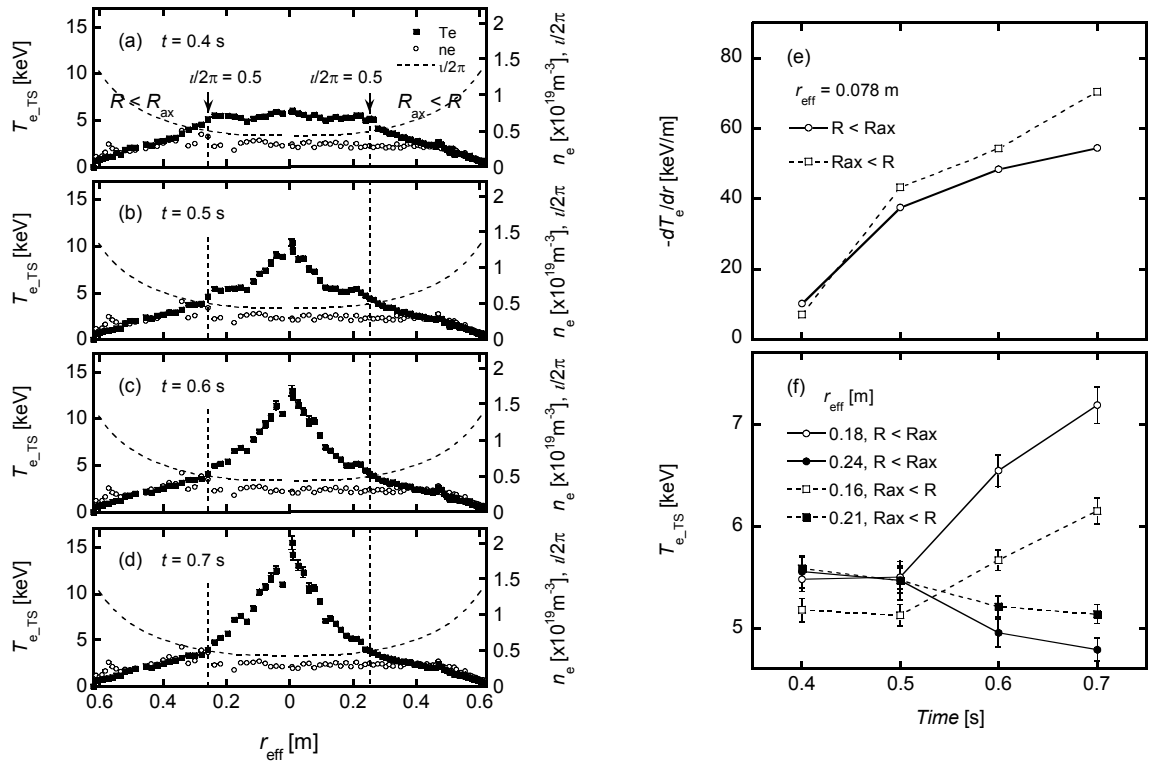

FIG. 7. The time evolution of (a)-(d) T_e, n_e profile, (e) T_e gradient at r_{eff} = 0.078 m and (f) T_e slightly inside the rational surface of $\iota/2\pi$ = 0.5.

Figure 7 shows the time evolution of (a)-(d) T_e and n_e profile, (e) T_e gradient at r_{eff} = 0.078 m and (f) T_e slightly inside the rational surface of $\iota/2\pi$ = 0.5 under R_{ax} = 3.53 m, B_0 = 2.705 T. The rotational transform profile for a vacuum condition is attached in (a)-(d) and the rational surface of $\iota/2\pi$ = 0.5 is located at r_{eff} ~0.25 m. ECRH was injected perpendicularly during t = 0.21-0.71 s with P_{ECRH} = 2.63 MW. Highly accurate T_e profiles were successfully obtained by the accumulation of the intensity of Thomson scattered light through 20 discharges with the three YAG lasers all injected together. At the beginning of the discharge, a flat T_e profile with a small bump was observed and a peaked T_e profile was formed at t = 0.5 s. After that the foot point of the e-ITB moved outward with increasing T_{e0}. As can be seen from Fig. 7 (a)-(d), steep gradient of T_e formed in the vicinity of the rational surface, which was larger than that in the e-ITB region. Fig. 7 (e) indicates that T_e at the core region increased with the foot point moving outward and the e-ITB growing such that the T_e gradient increased during the discharge. On the other hand, T_e just inside the rational surface (at r_{eff} = 0.21 and 0.24 m) gradually decreased as shown in Fig. 7 (f) leading to the increase of the T_e gradient at the core region and to the decrease of that around the rational surface. Finally, the T_e gradient at the e-ITB region equated with that around the rational surface indicating that (i) the foot point of the e-ITB reached to the position of the rational surface of $\iota/2\pi$ = 0.5 and (ii) the e-ITB plasma with only one folding point in its T_e profile was formed. We also observed same T_e profile behavior in higher density plasmas up to $n_e = 0.73\times10^{19}$ m^{-3}.

5. Summary

We investigated the confinement characteristics of the high T_e, low collisional plasmas produced by high power ECRH in LHD. Highly accurate high-T_e profiles were successfully obtained by the accumulation of the intensity of Thomson scattered light by fixed shot accumulation and the simultaneous firing with three YAG lasers. The configuration survey was carried out and the highest T_e and the steepest profile were obtained for the configuration of R_{ax} = 3.53 m, which is predicted as the optimum condition in the view point of neoclassical transport. Clear n_e threshold (and/or P_{ECRH}/n_e threshold) for the formation of the e-ITB was observed. The T_e profile drastically changed from flat to peaked one in the narrow n_e range and the E_r made a transition from negative to positive at the core region. Once the e-ITB formed, T_{e0} increased with the proportional dependence of $\sim(P_{ECRH}/n_e)^{0.5}$ and finally more than 15 keV of T_{e0} was successfully achieved. We investigated the formation process of the e-ITB structure for a high T_e, low collisional plasma. The foot point of an e-ITB moved outward during the ECRH injection and the flat T_e profile gradually healed with the propagation of the e-ITB foot point. We found that the increase of T_e at the core region was due to the foot point moving outward and the e-ITB growing. The foot point finally reached to a lower order rational surface of $\iota/2\pi$ = 0.5 and the e-ITB plasma with only one folding point in its T_e profile was formed.

References

[1] FUJITA T. et al., “Formation conditions for electron internal transport barriers in JT-60U plasmas”, Plasma Phys. Control. Fusion **46** (2004) A35.

[2] FUJISAWA A., “Experimental Studies of Structural Bifurcation in Stellarator Plasmas”, Plasma Phys. Control. Fusion **45** (2003) R1.

[3] BURATTI P. et al., “High Core Electron Confinement Regimes in FTU Plasmas with Lowor Reversed-Magnetic Shear and High Power Density Electron-Cyclotron-Resonance Heating”, Phys. Rev. Lett. **82** (1999) 560.

[4] FUJISAWA A. et al., "Electron Thermal Transport Barrier and Density Fluctuation Reduction in a Toroidal Helical Plasma", Phys. Rev. Lett. **82** (1999) 2669.
[5] PIETRZYK Z. A. et al., "Long-Pulse Improved Central Electron Confinement in the TCV Tokamak with Electron Cyclotron Heating and Current Drive", Phys. Rev. Lett. **86** (2001) 1530.
[6] IDA K. et al., "Characteristics of Electron Heat Transport of Plasma with an Electron Internal-Transport Barrier in the Large Helical Device", 2003 Phys. Rev. Lett. **91** (2003) 085003.
[7] KOIDE Y. et al., "Comparison of internal transport barriers in JT-60U and DIII-D NCS discharges", Plasma Phys. Control. Fusion **40** (1998) 97.
[8] JOFFRIN E. et al., "Internal transport barrier triggering by rational magnetic flux surfaces in tokamaks", Nucl. Fusion **43** (2003) 1167.
[9] CASTEJ´ON F. et al "Influence of low-order rational magnetic surfaces on heat transport in TJ-II heliac ECRH plasmas", 2004 Nucl. Fusion **44** (2004) 593.
[10] SHIMOZUMA T. et al., "Transition phenomena and thermal transport properties in LHD plasmas with an electron internal transport barrier", Nucl. Fusion **45** (2005) 1396.
[11] TAKAHASHI H. et al., "The Development of a 77-GHz, 1-MW ECRH System for the Large Helical Device", Fusion Sci. Technol. **57** (2010) 19.
[12] KUBO S. et al., "Extension and characteristics of an ECRH plasma in LHD", Plasma Phys. Control. Fusion **47** (2005) A81.
[13] TAKEIRI Y. et al., "Electron ITB Formation with Combination of NBI and ECH in LHD", Fusion Sci. Technol. **46** (2004) 106.
[14] IDA K. et al., "Bifurcation Phenomena of a Magnetic Island at a Rational Surface in a Magnetic-Shear Control Experiment", Phys Rev. Lett. **100** (2008) 045003.
[15] YAMADA H. et al., "Energy confinement and thermal transport characteristics of net current free plasmas in the Large Helical Device", Nucl. Fusion **41** (2001) 901.
[16] SHIMOZUMA T. et al., "ECRH-Related Technologies for High-Power and Steady State Operation in LHD", Fusion Sci. Technol. **58**, (2010) 530.
[17] YAMADA I. et al., "Improvements of data quality of the LHD Thomson scattering diagnostics in high-temperature plasma experiments", submitted to Rev. Sci. Instrum.
[18] MURAKAMI S. et al., "Neoclassical transport optimization of LHD", Nucl. Fusion **42** (2002) L19.
[19] MURAKAMI S. et al., "Effect of neoclassical transport optimization on electron heat transport in low-collisionality LHD plasmas", Fusion Sci. Technol. **51** (2007) 112.
[20] KUBO S. et al., "ECRH and ECE in high T_e, low density plasmas of LHD", proc. 16th Joint Workshop on ECE and ECRH, April 12-15, 2010, Sanya, China.
[21] BEIDLER C.D. and D'HAESELEER W.D., "A general solution of the ripple-averaged kinetic equation (GSRAKE)", Plasma Phys. Control. Fusion **37** (1995) 463.
[22] MATSUOKA S. et al., "Neoclassical Transport Properties in High-Ion-Temperature Hydrogen Plasmas in the Large Helical Device (LHD)", Plasma and Fusion Research **3** (2008) S1056.
[23] YOKOYAMA M. et al., "Core electron-root confinement (CERC) in helical plasmas", Nucl .Fusion **47** (2007) 1213.
[24] IDO T. et al., "6 MeV heavy ion beam probe on the Large Helical Device", Rev. Sci. Instrm. **77** (2006) 10F523.